

## Silencing NEAT1 suppresses thyroid carcinoma via miR-126/NEAT1/VEGFA axis

Weiwei Zeng<sup>1</sup>, Yan Lin<sup>1</sup>, Hai Lin, Xuemei Wu<sup>1</sup>

<sup>1</sup>Department of Endocrinology, Rui'an People's Hospital and The Third Affiliated Hospital of Wenzhou Medical University, rui'an, Zhejiang, 325200, P. R. China

### TABLE OF CONTENTS

1. Abstract
2. Introduction
3. Material and methods
  - 3.1. Reagents
  - 3.2. Cell culture
  - 3.3. Cell transfection
  - 3.4. qPCR
  - 3.5. Luciferase reporter assay
  - 3.6. BrdU labeling and staining
  - 3.7. Transwell culture
  - 3.8. Scratch test
  - 3.9. Flow cytometry
  - 3.10. Western blotting
  - 3.11. RNA Binding-Protein Immunoprecipitation (RIP) assay
  - 3.12. Pull down assay
  - 3.13. Establishment of xenograft mouse model
  - 3.14. Immunohistochemistry
  - 3.15. Statistic analysis
4. Results
  - 4.1. NEAT1 is highly expressed in thyroid cancer cells and knockdown of NEAT1 inhibits cell growth and promotes cell apoptosis
  - 4.2. Knockdown of NEAT1 inhibits migration and epithelial-mesenchymal transition (EMT)
  - 4.3. miR-126 targets and negatively regulates NEAT1
  - 4.4. miR-126 regulates VEGFA expression, cell growth and motility and apoptosis
  - 4.5. Silencing NEAT1 down-regulates VEGFA level, increases apoptosis and inhibits tumor cell growth *in vivo*
5. Discussion
6. Acknowledgments
7. References

**1. ABSTRACT**

The incidence of papillary thyroid carcinoma (PTC) has steadily increased over the recent years, making this cancer a common malignant tumor world-wide. We tested the

hypothesis that Nuclear Enriched Abundant sh-NEAT1 knock-down transcript 1 (NEAT1) is involved in the pathogenesis of PTC *in vitro* and *in vivo*. We show that NEAT1 is highly expressed in Papillary

Thyroid Carcinoma cell line (PTC-1) and anaplastic thyroid cancer cell line (SW1736) as compared with the human thyroid follicular epithelial cell line (Nthy-ori 3-1). shRNA knockdown of NEAT1 led to the inhibition of cell growth, invasion, migration and **Epithelial to Mesenchymal Transition (EMT)** of thyroid cancer cells. This treatment increased the rate of apoptosis in SW1736 cells. Silencing of NEAT1 increased the level of its regulator, miRNA-126 and down-regulated VEGFA that sets the density of tumor vasculature. Administration of sh-NEAT1 also inhibited tumor growth *in vivo*, increased the miRNA-126 level and down-regulated VEGFA. Taken together, these results indicate that silencing NEAT1 suppresses thyroid carcinoma via miR-126/NEAT1/VEGFA axis.

## 2. INTRODUCTION

Papillary thyroid carcinoma (PTC) is a common malignant tumor worldwide, and its incidence has steadily increased over the past few decades. Recurrence or metastasis occurs in about 10% of the cases within 10 years after operation (1-3). Treatment with radioactive iodine combined with levothyroxine has improved the prognosis, however, these treatments were far from being effective in cure necessitating development of more effective treatment strategies.

Long-chain non-coding RNAs (LncRNA) were aberrantly overexpressed in various tumors and available evidence suggests that these RNAs regulate cell proliferation, invasion and metastasis of diverse tumors (4-5). As a prototypical LncRNAs, Nuclear Enriched Abundant Transcript 1 (NEAT1), has been shown to regulate growth, apoptosis, invasion and metastasis of various cancer cells, and for this reason, NEAT1 might serve as a potential target for development of cancer treatment (6). For example, in non-small cell lung cancer (NSCLC) cell line, NEAT1 was up-regulated, and down-regulation of its expression inhibited the tumor progression (7). Similarly, in PTC, NEAT1 or 2 were up-regulated and their silencing inhibited the growth and motility of cancer cells, reduced apoptosis and lowered the resistance of cancer cells to radioactive iodine (8). NEAT1 appears to regulate the tumor progression in PTC through miRNAs such as miR-101-3p or miR-

129 (9). Another candidate miRNA that might regulate NEAT1 is miR-126 with effects on growth, invasion, migration and apoptosis. For example, miR-126 is underexpressed in PTC and its overexpression has been shown to inhibit proliferation by targeting LRP6, and to induce apoptosis by reducing the level of VEGFA (10-19). Based on such evidence, we tested the hypothesis that NEAT1 and miR-126 are involved in the pathogenesis of PTC *in vitro* and *in vivo*.

## 3. MATERIAL AND METHODS

### 3.1. Reagents

RPMI-1640 cell culture medium, 0.25% trypsin and fetal bovine serum (FBS) were from Gibco (USA). MiR-126 mimics, miR-126, shRNA-NC and sh-NEAT1 were designed and synthesized by Shanghai GenePharma Co., Ltd. Lipfectamine 2000 transfection, TRIzol and reverse transcription kits were from Thermo-Fisher Company (USA), primary and secondary antibodies were from Abcam (UK), RIPA buffer was from Sigma-Aldrich (USA), BCA kit was from Beyotime Biotechnology, Dual-Luciferase® Reporter assay kit was from Promega (USA), Edu kit was from Guangzhou RiboBio Co., Ltd, Matrigel was from Invitrogen (USA). Anti-BrdU antibody was from (Biocompare, San Francisco, CA). Secondary antibody was obtained from Thermo-Fisher (USA).

### 3.2. Cell culture

Human papillary thyroid carcinoma cell line (PTC-1), anaplastic thyroid cancer cell line (SW1736) and the normal thyroid cell line (Nthy-ori 3-1) were purchased from the cell bank of the Chinese Academy of Medical Sciences. When the fusion rate reached 85% or more, cells were cultured in a 5% CO<sub>2</sub> incubator at 37 ° C in RPMI-1640 medium supplemented with 10% FBS. Cell suspensions in complete medium were introduced at a density of 2 × 10<sup>7</sup>/ml to animals.

### 3.3. Cell transfection

Cells were cultured in 12-well plates at a cell density of 1 × 10<sup>6</sup> ml. After 24 hours of culture,

**Table 1.** Sequences of primers and shRNA

Gene	Sense 5'-3'	Antisense 5'-3'
β-actin	TGACCAATTGCC GAATGC	CCAATGCATGGCATTAGCC
NEAT1	GATCCCAGATGGG TCATCC	GGTAAACTACATTGACG
miR-126	GCTTCGAATCGC CCGGGG	TACCGATTGACCGCGGATTG
VEGFA	TCAGGCTTGAACG ACTTGC	CTGGACGGTTAACGGCACG

cells were transfected using Lipofectamine 2000 according to the manufacturer's instructions. Cells were transfected with shRNAs to NEAT1 (TGGCTAGCTCAGGGCTTCAG) which was inserted into the lentivirus core vector (hU6-MCS-CMV-RFP, GeneChem, Shanghai, China). Four hours later, cells were washed, cultured in culture medium, and incubated for an additional 48 hours before they were tested.

#### 3.4. qPCR

Total RNA was extracted from cells or tumor tissues with Trizol reagent. cDNAs of NEAT1, miR-126 and VEGFA were synthesized using a reverse transcription kit. RT-qPCR was performed using primers (Table 1) using the ABI 7500 Real-Time PCR System (Applied Biosystems, USA) with the FastKing One Step RT-qPCR kit according to the manufacturer's protocol. The primers used in the experiment were designed and synthesized by Sangon Biotech Co., Ltd. β-actin was used as an internal reference. Fold changes were calculated by the equation  $2^{-\Delta\Delta Ct}$ .

#### 3.5. Luciferase reporter assay

The bioinformatics analysis software, TargetScan7.0 (<http://www.targetscan.org>), was used to predict the potential binding sites of miR-126 to NEAT1. Then, wild and mutant NEAT1 were amplified by PCR and the amplified fragments were inserted into pcDNA vector to construct wild type and NEAT1 mutant type plasmid. PTC-1 cells were transfected with wild or mutant plasmids alone or with miR-126 mimic. Luciferase activity was measured

according to manufacturer's instruction.

#### 3.6. BrdU labeling and staining

PTC-1 and SW1736 cells were introduced into 96-well plates in a total volume of 200 μl per well and cultured overnight and these were incubated with BrdU (10 μg/mL) for 1 hour, after which the cells were fixed in 4% paraformaldehyde for 10 min and stained with an anti-BrdU antibody according to the manufacturer's instructions. Cells were counterstained with DAPI and photographed with a fluorescence microscope (Olympus, Tokyo, Japan).

#### 3.7. Transwell culture

Migration of cells was examined in Matrigel-coated transwell chambers. Cells were pre-cultured in the upper well at a density of  $4 \times 10^5$  cells/ml. Cells were then cultured in medium alone while the lower chamber received normal cell culture medium with fetal bovine serum. After 48 hours of continuous culture, cells in the upper chamber bound to the matrigel were removed using a sterile cotton swab. Then, the cells that migrated through the membrane layer were stained with crystal violet. Five different fields of view were randomly selected for cell count. The experiment was repeated at least 3 times with 6 replicate wells per group.

#### 3.8. Scratch test

PTC-1 or SW1736 cells were seeded at a density of  $1 \times 10^6$  cells/ml in triplicates in sterile 12-well plates. After cells attached to the culture dishes, cell cultures were scratched with five straight lines and the number of cells that migrated into the scratched lines were counted under a microscope.

#### 3.9. Flow cytometry

PTC-1 or SW1736 cells were seeded in 6-well plates at a density of  $1 \times 10^5$  cells/ml. When the dishes reached 80% or more confluence, cells were removed by incubation with 0.25% trypsin, washed and suspended in medium at a density of  $1 \times 10^6$  cells/ml. Cells were stained with FITC-Annexin V kit, counterstained with propidium iodide and kept for 15 minutes in the dark before

they were subjected to flow cytometric analysis.

### 3.10. Western blotting

Proteins were extracted with RIPA buffer on ice and histone concentration was determined using a BCA kit. Proteins were resolved in 12% SDS-PAGE, and transferred to a PVDF membrane. Membranes were blocked with 5% skim milk powder for 2 h at room temperature, were incubated overnight at 4° C with primary antibodies (1 µg/ml) and washed with buffer before appropriate secondary antibodies were applied at room temperature for 1 h. Membranes were then washed and incubated with ECL in the dark. β-actin was used as a housekeeping control.

### 3.11. RNA Binding-Protein Immunoprecipitation (RIP) assay

RNA-protein complexes were isolated in complete RIP lysis buffer and RNA immunoprecipitation was performed using a Magna RIP™ RNA-Binding Protein Immunoprecipitation Kit (Millipore, Billerica, MA, USA) according to the manufacturer's protocol. RNA-protein complexes were, then, digested with proteinase K with constant shaking and immunoprecipitated RNAs were isolated. The concentration of RNA was measured using a NanoDrop (Thermo Scientific), and the RNA quality was assessed using a bioanalyzer (Agilent, Santa Clara, CA, USA). Purified RNA were subjected to qPCR.

### 3.12. Pull down assay

RNA pull down assay was performed as previously described (20). NEAT1-wt, NEAT1-mut, VEGFA-wt and VEGFA-mut were transcribed from the vector pGEM®-T (Promega Corporation). RNAs were labeled with a biotin RNA labeling mixture (Hoffman-La Roche Ltd., Basel, Switzerland). T7 RNA polymerase was treated with RNase-free DNase I (Hoffman-La Roche Ltd.) and purified using RNeasy Mini Kit (Qiagen, Valencia, CA, USA). Biotinylated NEAT1 and VEGFA probes were dissolved in binding and wash buffers, and then these were incubated with Dynabeads M-280 streptavidin (Thermo Fisher Scientific) for 10 min at 25° C to

generate probe-coated beads according to the manufacturer's protocol. Then, cell lysates were incubated with probe-coated beads. RNA complexes bound to these beads were extracted for qPCR analysis.

### 3.13. Establishment of xenograft mouse model

Sixty five week old SCID nude mice were purchased from Beijing Vital River Laboratory Animal Technology Co., Ltd, housed in a sterile environment at 26-28° C. One week prior to each experiment, mice were fed freely with sterile water and food. Then, PTC-1 cells ( $2 \times 10^7$ /ml) transfected either with sh-NEAT1 or with control medium were injected subcutaneously into the neck of mice and survival rates were assessed continuously for 30 days. The tumor volumes were measured every 5 days and the tumor tissues were weighed at the end of the experiment. Tumor volume and survival rates were calculated as follows.

$$\text{Tumor volume} = \text{Tumor diameter} \times \text{width}^2$$

$$\frac{2}{2}$$

$$\text{Survival rate} = \frac{\text{Number of surviving mice}}{\text{No. of mice in each group}} \times 100\%.$$

### 3.14. Immunohistochemistry

Paraffin sections were deparaffinized in xylene, rehydrated in gradients of ethanol, incubated for 30 minutes in 30% H<sub>2</sub>O<sub>2</sub> and then these section were incubated overnight with primary antibodies at 4° C. After washing three times with TBST, sections were incubated with Alexa Fluor 488 labeled secondary antibody (2 µg/ml) for 3 hours at room temperature.

### 3.15. Statistic analysis

Data analysis was carried out using SPSS 19.0 statistic software, and statistical analysis was done using the t-test or one-way ANOVA. The experimental data were expressed

as means  $\pm$  standard deviation, with a p value of  $< 0.05$  being considered as significant.

#### 4. RESULTS

##### 4.1. NEAT1 is highly expressed in thyroid cancer cells and knockdown of NEAT1 inhibits cell growth and promotes cell apoptosis

The expression of NEAT1 in PTC-1 and SW1736 thyroid cancer cell lines was significantly higher than that in Nthy-ori3- 1 normal control group (Figure 1A). In PTC-1 and SW1736 cells, sh-NEAT1 knock-down significantly decreased the expression of NEAT1, reduced Ki67 and cell growth, and increased caspase 3 and apoptosis of these cells (Figure 1A-E).

##### 4.2. Knockdown of NEAT1 inhibits migration and epithelial-mesenchymal transition (EMT)

The healing rate of scratches introduced in PTC-1 and SW1736 cultures were not significantly different after transfection of shRNA-NC from that of the control group is ( $p > 0.05$ ). However, the healing rate of cells transfected with sh-NEAT1 was significantly lower than those obtained in shRNA-NC and control group (Figure 2A). The rate of migration through transwells was also not different in shRNA-NC group and control group. However, in cells treated with sh-NEAT1 group this rate was significantly reduced as compared with rates quantitated in shRNA-NC and control group (Figure 2B). While, the expression of invasion markers including E-cadherin, N-cadherin and Vimentin in shRNA-NC group was not significantly different from that in control group, E-cadherin expression increased and N-cadherin and Vimentin were significantly reduced in cells that were treated with sh-NEAT1 (Figure 2C).

##### 4.3. miR-126 targets and negatively regulates NEAT1

Figure 3A shows the results of predictions based on bioinformatics. To validate such findings,

the expression of miR-126 was significantly lower in PTC-1 and SW1736 cells than that in Nthy-ori3-1 group (Figure 3B) While, there was no significant difference between shRNA-NC group and control group ( $p > 0.05$ ), miR-126 expression was significantly up-regulated in cells transfected with sh-NEAT1 (Figure 3C). Luciferase reporter assays, RNA immunoprecipitation and RNA pull down assays further confirmed the direct interaction of NEAT1 with miR-126 (Figure 3D, E and F).

##### 4.4. miR-126 regulates VEGFA expression, cell growth and motility and apoptosis

Bioinformatics prediction revealed existence of a VEGFA binding site in the miR-126 gene (Figure 4A). While there was no significant change in the expression of VEGFA in PTC-1 and SW1736 after shRNA-NC transfection, after sh-NEAT1 transfection, the level of VEGFA was significantly lower than that in shRNA-NC and control groups (Figure 4B). Silencing of NEAT1 also significantly reduced whereas inhibition of miR-126 inhibitor increased VEGFA level (Figure 4C). miR-126 mimic amplified the inhibitory effect of NEAT1 silencing on VEGFA expression (Figure 4C).

Functional experiments show that knockdown of NEAT1 induced apoptosis and significantly inhibited cell growth, invasion, migration and EMT (Figure 4D-4K). These effects could be counteracted with miR-126 inhibitor (Figure 4D-4G).

##### 4.5. Silencing NEAT1 down-regulates VEGFA level, increases apoptosis and inhibits tumor cell growth *in vivo*

The rate of apoptosis was higher, expression of Ki67 was lower and tumor volumes and weights were significantly reduced in sh-NEAT1 transfected tumor-bearing mice as compared to the control group (Figure 5). The expression of NEAT1, VEGFA, N-cadherin, Snail and Vimentin was significantly lower and miR-126 level was significantly higher in tumor tissues of sh-NEAT1 group as compared to those in the control tumors (Figure 5).

### shNEAT1 inhibits PTC via sponging miR-126

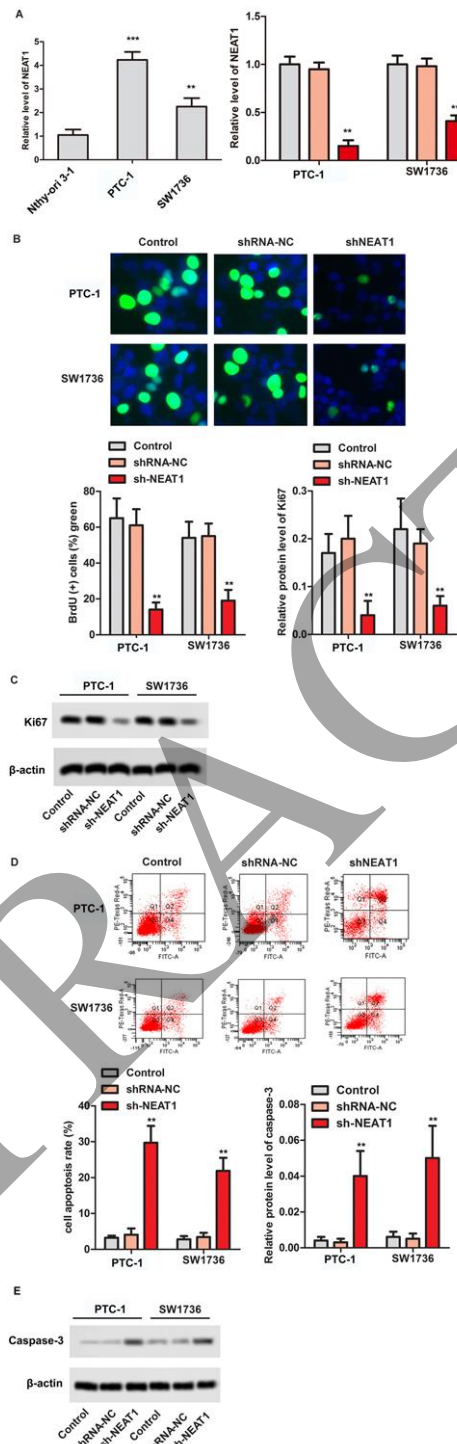


**Figure 1.** NEAT1 is highly expressed in thyroid cancer cells and knockdown NEAT1 inhibits cell growth and promotes cell apoptosis. PTC-1 and SW1736 cells are transfected with shRNA-NC or sh-NEAT1. A. The mRNA levels of NEAT1 in Nthy-ori3-1, PTC-1 and SW1736 cells are detected by RT-qPCR. B. Cell growth of PTC-1 and SW1736 is detected by BrdU staining. C and E. The protein level of Ki67 and Caspase3 are detected by western blotting. D. Cell apoptosis rates of PTC-1 and SW1736 are detected by flow cytometry assay. (\*\* p < 0.01 vs the control group).

## shNEAT1 inhibits PTC via sponging miR-126

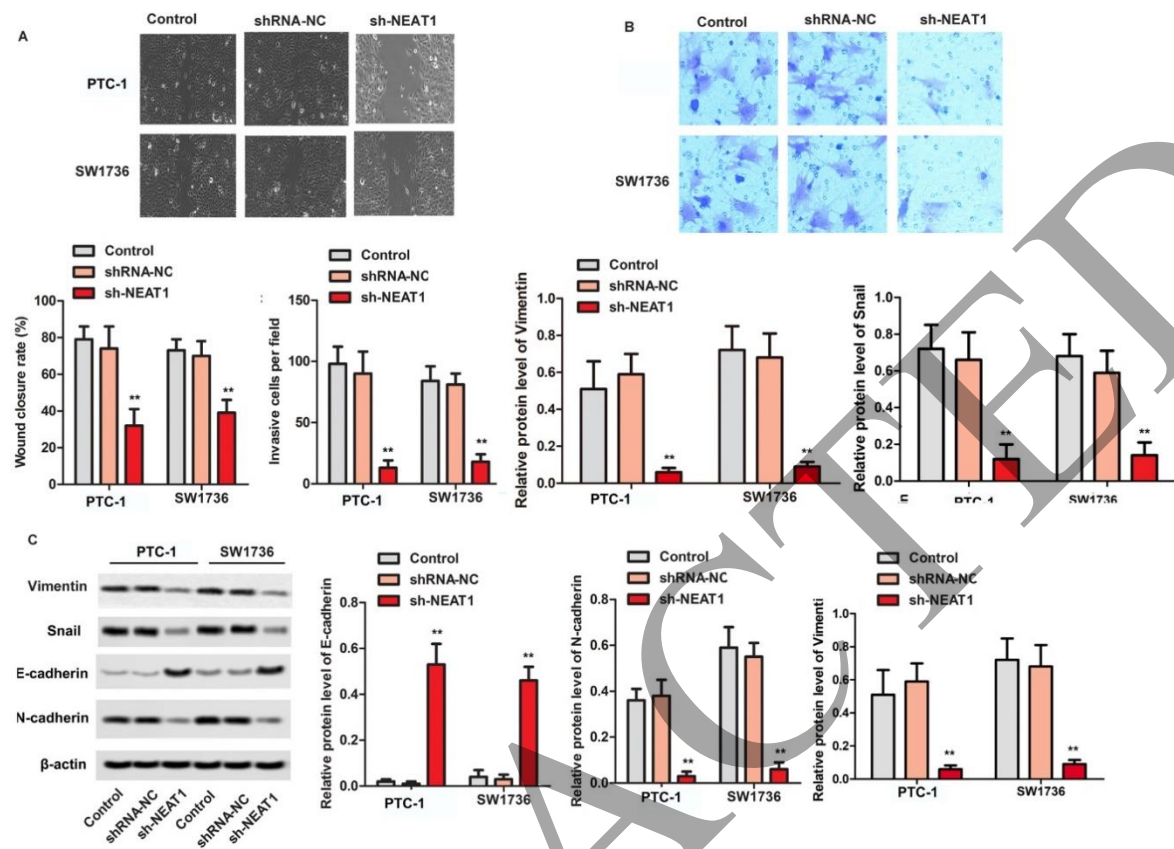


**Figure 2.** Knockdown of NEAT1 inhibits invasion, migration and epithelial-mesenchymal transition (EMT) of PTC-1 and SW1736 cells *in vitro*. PTC-1 and SW1736 cells are transfected with shRNA-NC or sh-NEAT1. A. Migratory ability of PTC-1 and SW1736 cells is measured by wound healing assay. B. Invasive ability of PTC-1 and SW1736 cells is measured by transwell assay. C. The protein levels of Vimentin, E-cadherin and N-cadherin are measured by western blotting. (\*\* p < 0.01 vs the control group).

## 5. DISCUSSION

The incidence of thyroid carcinoma has been on the rise (21) and while early detection leads to better prognosis, when the diagnosis is not made early, the tumor can lead to epidural infiltration, lymph node metastasis and distant metastasis (22). Therefore, understanding the mechanism of such invasion and metastasis has the potential to improve the outcome of this disease.

NEAT1, is overexpressed in many cancers including tumors that arise from the lung, breast, liver and colorectum (23). NEAT1 is considered as oncogene as its knockdown has been shown to inhibit the colorectal cancer growth by regulating the miR-1mRNA-3p/KRAS axis (23). In PTC, NEAT1 and 2 are overexpressed and their knockdown inhibits the

growth and motility and decreases the resistance of PTC cells through the miR-101-3p/FN1/PI3K-AKT axis (8). Another pathway that is involved in NEAT1 signaling has been shown to involve miR-129-5P/KLK7 axis (9). NEAT1 also has been shown to promote proliferation, invasion and EMT of osteosarcoma cells *in vivo*, likely by impacting the miR-186-5P/HIF1  $\alpha$  axis (24).

More than 60% of miRNA binding sites in human protein coding genes play an important role in cell growth, proliferation, apoptosis and migration. miRNAs affect tumorigenesis and tumor development by regulating the expression of protein coding genes (25-26). Among the miRNAs, the expression of miR-126 is altered in various cancers including PTC (27). Furthermore, forced over-expression of miR-126 can lead to slowed G1 phase,

### shNEAT1 inhibits PTC via sponging miR-126

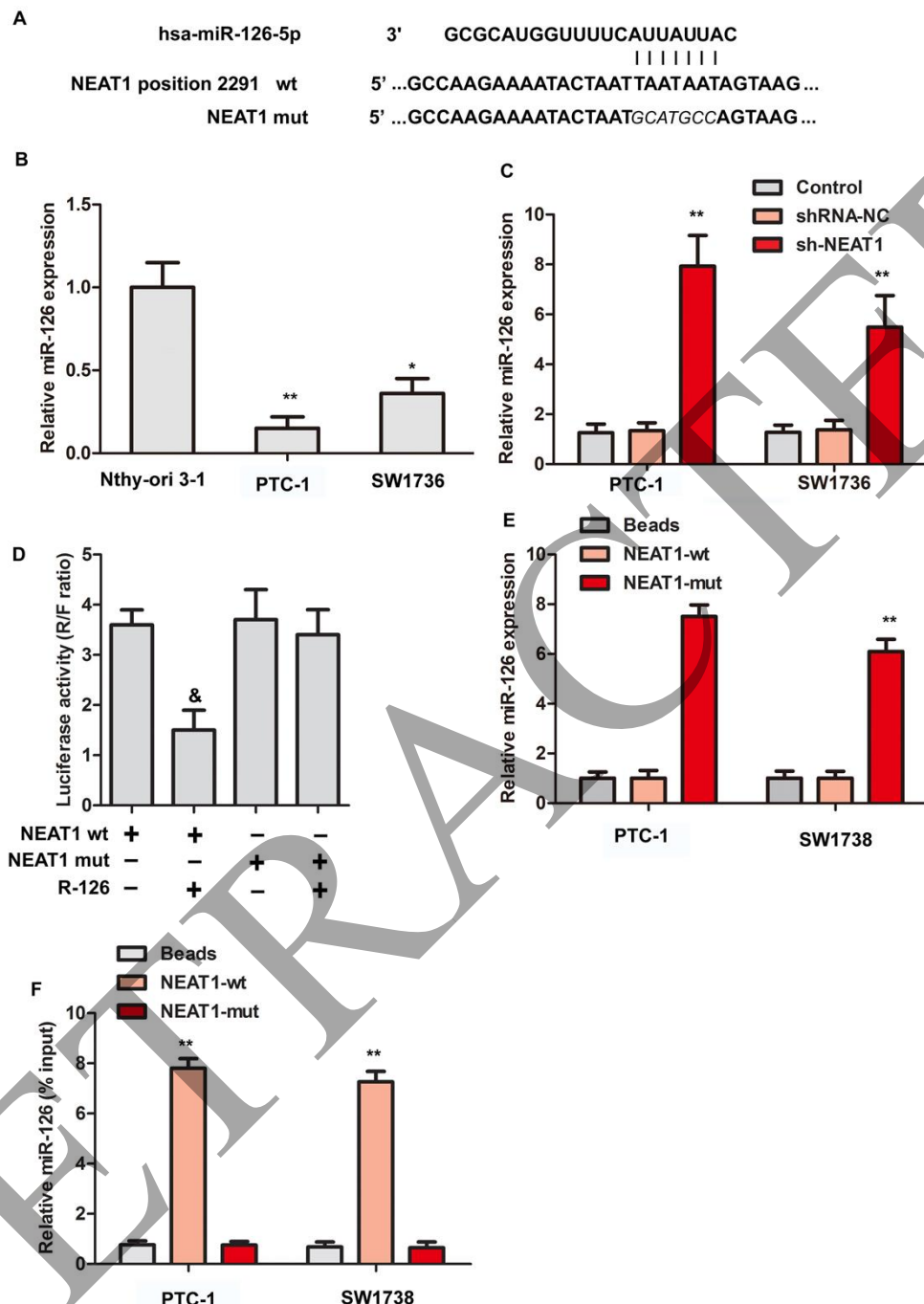


**Figure 3.** MIR-126 targets NEAT1 and negatively regulates NEAT1. A. The target relationship between miR-126 and NEAT1 is predicted by Targetscan7.0. B. The mRNA levels of miR-126 in Nthy-ori3-1, PTC-1 and SW1736 cells are detected by RT-qPCR. (\*\*p < 0.02 vs the control group) C. PTC-1 and SW1736 cells are transfected with shRNA-NC or sh-NEAT1. The mRNA level of miR-126 in each group is detected by RT-qPCR. D. PTC-1 cells are transfected with NEAT1 wt or NEAT1 mut alone or in combination with miR126 mimic. Luciferase activity is detected by luciferase reporter assay. (&p < 0.05 vs NEAT1 wt group) E. RNA levels in immunoprecipitates are determined by qRT-PCR. (\*\*p < 0.02 vs the control group) F. Cell lysates are harvested from PTC-1 and SW1736 cells and incubated with biotin-labeled NEAT1-wt and NEAT1-mut individually. Subsequently, a RT-qPCR assay is performed to measure the pulled-down miR-126 in each group. (\*\*p < 0.02 vs Beads).

## shNEAT1 inhibits PTC via sponging miR-126

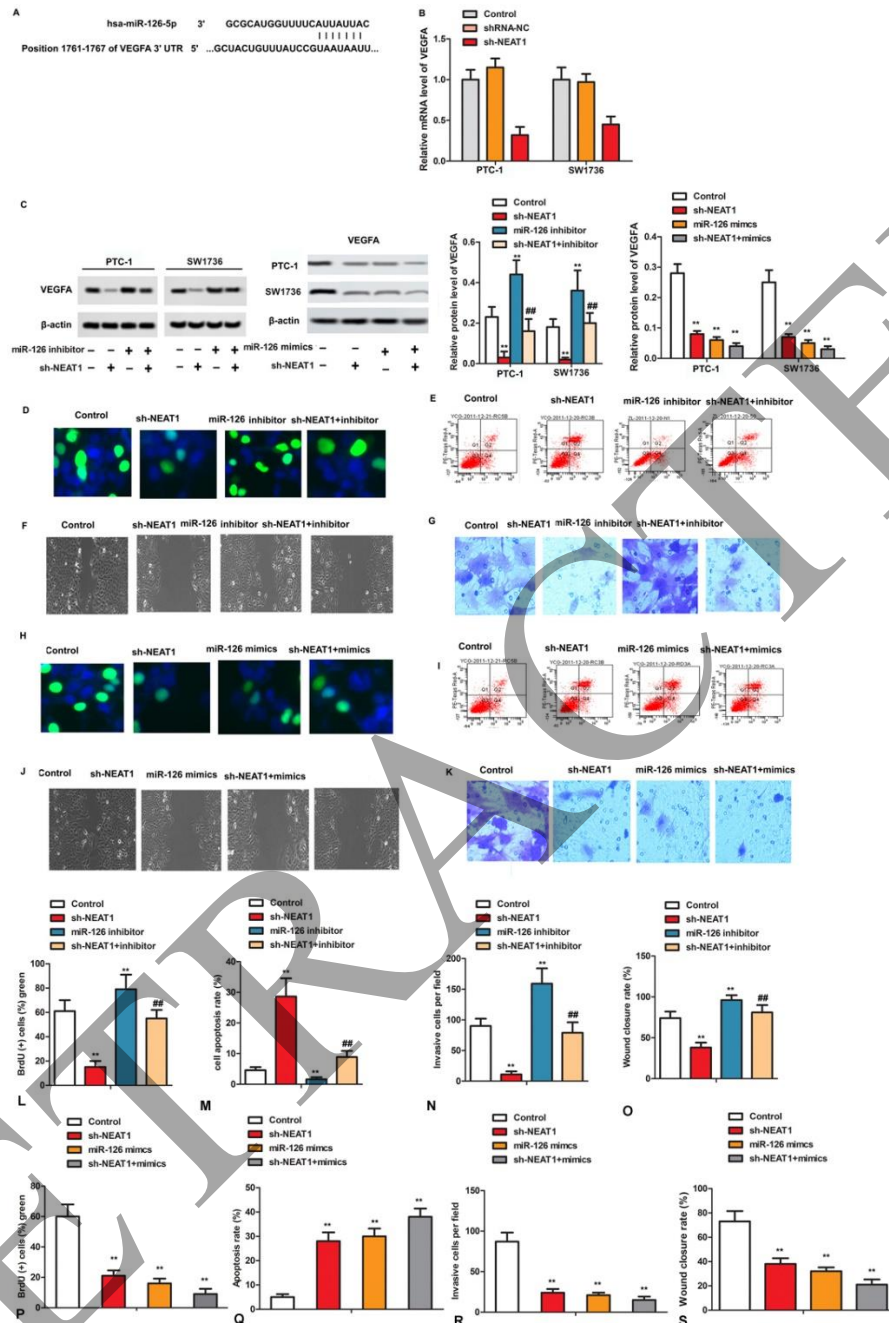


**Figure 4.** MiR-126 inhibits cell growth and motility and induces apoptosis by down-regulating VEGFA levels. **A.** The target relationship between miR-126 and VEGFA is predicted by Targetscan7.0. **B.** PTC-1 and SW1736 cells are transfected with shRNA-NC or sh-NEAT1. The mRNA level of VEGFA is detected by RT-qPCR. **C.** PTC-1 and SW1736 cells are transfected with miR-126 inhibitor, miR-126 mimic and / or sh-NEAT1. The protein level of VEGFA is detected by western blotting. **D-G.** PTC-1 and SW1736 cells are transfected with miR-126 inhibitor and / or sh-NEAT1. **D.** Cell growth is detected by BrdU staining. **E.** Cell apoptosis rate is detected by flow cytometry assay. **F.** Migrative ability is measured by wound healing assay. **G.** Invasive ability is measured by transwell assay. **H-K.** PTC-1 and SW1736 cells are transfected with miR-126 mimic and / or sh-NEAT1. **H.** Cell growth is detected by BrdU staining. **I.** Cell apoptosis rate is detected by flow cytometry assay. **J.** Migrative ability is measured by wound healing assay. **K.** Invasive ability is measured by transwell assay. **L-S.** Quantitative analysis of D - K. (\* p < 0.01 vs the control group; \*\* p < 0.01 vs miR-126 inhibitor group).

### shNEAT1 inhibits PTC via sponging miR-126

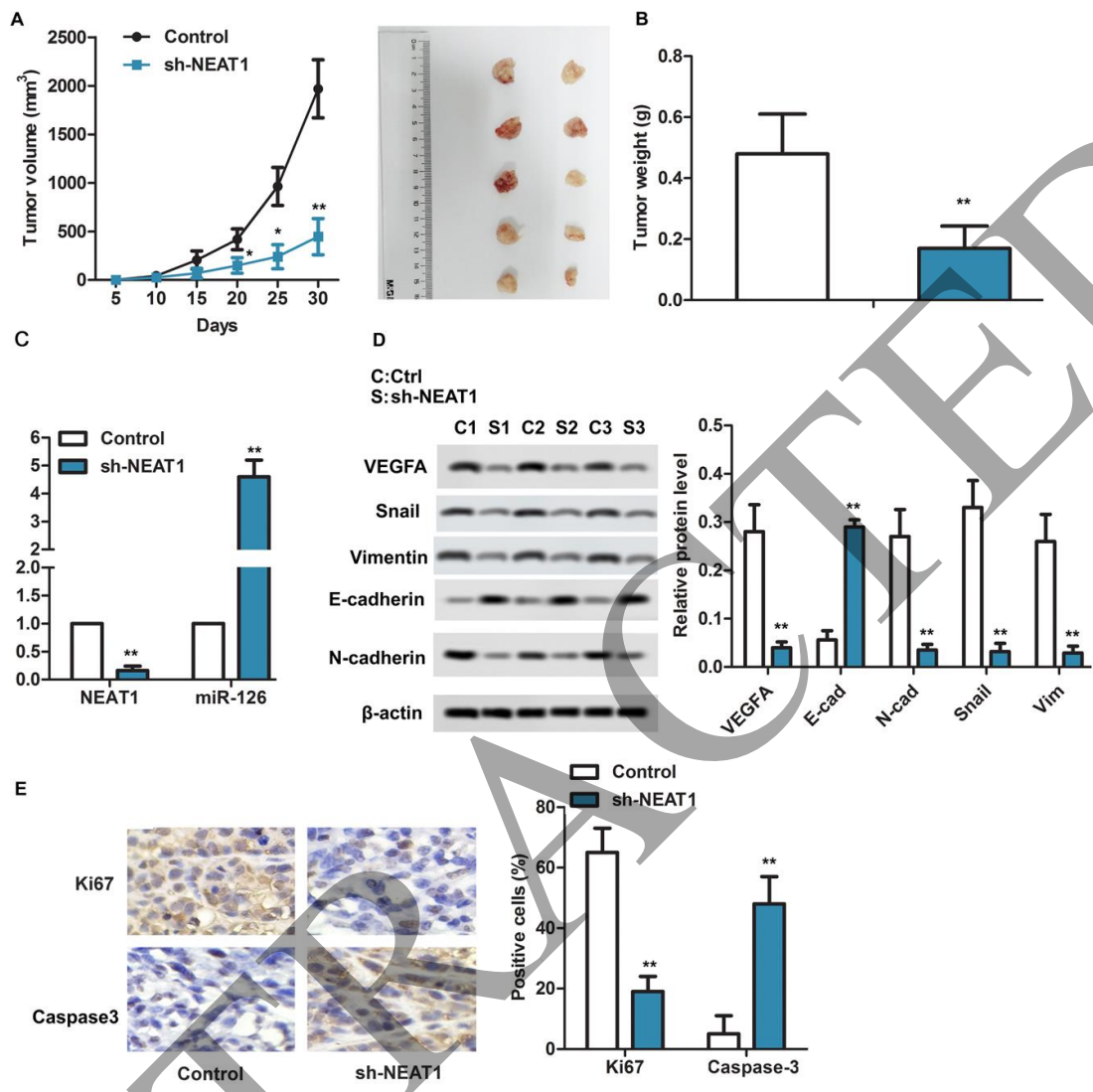


**Figure 5.** Silencing NEAT1 inhibits tumor cell growth and motility by down-regulating VEGFA level *in vivo*. After successful modelling, the mice are divided into two groups ( $n = 10$ ): Control group and sh-NEAT1 group. A. Tumor volume. B. Tumor weight. C. The mRNA levels of NEAT1 and miR-126 are detected by RT-qPCR. D. The protein levels of VEGFA, Snail, Vimentin, E-cadherin and N-cadherin are detected by western blotting. E. The expression levels of Ki67 and Caspase3 are detected by IHC. (\*\* $p < 0.01$  vs the control group).

inhibition of cell proliferation, migration and invasion, and apoptosis *in vitro* and reduced tumor growth *in vivo* (19). Consistent with such results, here, we show that NEAT1 is highly expressed in papillary thyroid carcinoma (PTC-1) and anaplastic thyroid cancer (SW1736) cells as compared to normal controls. Knockdown of NEAT1 with shRNA leads to the inhibition of cell growth, invasion, migration and epithelial to mesenchymal transition (EMT) of cancer cells. This treatment also increases the rate of

apoptosis in SW1736 cells. Silencing of NEAT1 increases the level of its regulator, miRNA-126 and down-regulates VEGFA that sets the density of tumor vasculature. Luciferase reporter assays, RNA immunoprecipitation and RNA pull down assays further confirm the direct interaction of NEAT1 with miR-126. In addition, sh-NEAT1 knock-down down-regulates the expression of VEGFA by up-regulating miR-126 level *in vitro* and leads to inhibition of tumor growth *in vivo*. Taken together, these results are

consistent with the idea that silencing NEAT1 suppresses thyroid carcinoma via miR-126/NEAT1/VEGFA axis. Therefore, NEAT1 may be an important prognostic indicator for progression of thyroid carcinoma and might be a candidate therapeutic target for this cancer.

## 6. ACKNOWLEDGMENTS

This work was supported by the Natural Science Foundation of Zhejiang Province (LY16H161043)

## 7. REFERENCES

1. R. L. Brown, J. A. de Souza, E. E. Cohen. Thyroid cancer: burden of illness and management of disease. *J Cancer.* 2, 193-199 (2011)  
DOI: 10.7150/jca.2.193
2. M. Nikiforova, Y. Nikiforov. Molecular genetics of thyroid cancer: implications for diagnosis, treatment and prognosis. *Expert Rev Mol Diagn.*, 8, 83-95 (2008)  
DOI: 10.1586/14737159.8.1.83
3. H. H. L. Ms, FRACS, K. Y. Wan, FRCR, M. S. Chung-Yau Lo, FRCS. Significance of Metastatic Lymph Node Ratio on Stimulated Thyroglobulin Levels in Papillary Thyroid Carcinoma after Prophylactic Unilateral Central Neck Dissection. *Ann Surg Oncol.*, 19, 1257-1263 (2012)  
DOI: 10.1245/s10434-011-2105-5
4. L. Yang, L. Xu, Q. Wang, M. Wang, G. An. Dysregulation of long non-coding RNA profiles in human colorectal cancer and its association with overall survival. *Oncol Lett.*, 12, 4068 (2016)  
DOI: 10.3892/ol.2016.5138
5. M. A. Smolle, T. Bauernhofer, K. Pummer, G. A. Calin, M. Pichler. Current Insights into Long Non-Coding RNAs (LncRNAs) in Prostate Cancer. *Int J Mol Sci.*, 18, 473 (2017)  
DOI: 10.3390/ijms18020473
6. S. Ghaforui-Fard, M. Taheri. Nuclear Enriched Abundant Transcript 1 (NEAT1): A long non-coding RNA with diverse functions in tumorigenesis. *Biomed Pharmacother.*, 111, 51-59 (2018)  
DOI: 10.1016/j.biopha.2018.12.070
7. F. Wu, Q. Mo, X. Wan, J. Dan, H. Hu. NEAT1/has-mir-98-5p/MAPK6 axis is involved in non-small-cell lung cancer (NSCLC) development. *J Cell Biochem.* 120:2836-2846 (2017)
8. W. Sun, X. Lan, H. Zhang, Z. Wang, W. Dong, L. He, T. Zhang, P. Zhang, J. Liu, Y. Qin. NEAT1\_2 functions as a competing endogenous RNA to regulate ATAD2 expression by sponging microRNA-106b-5p in papillary thyroid cancer. *Cell Death Dis.*, 9, 380 (2018)  
DOI: 10.1038/s41419-018-0418-z
9. H. Zhang, Y. Cai, L. Zheng, Z. Zhang, X. Lin, N. Jiang. Long noncoding RNA NEAT1 regulate papillary thyroid cancer progression by modulating miR-129-5p /KLK7 expression. *J Cell Physiol.*, 233(10):6638-6648 (2018)  
DOI: 10.1002/jcp.26425
10. C. Zhao, Y. Li, M. Zhang, Y. Yang, L. Chang. miR-126 inhibits cell proliferation and induces cell apoptosis of hepatocellular carcinoma cells partially by targeting Sox2. *Human Cell*, 28, 91-99 (2015)  
DOI: 10.1007/s13577-014-0105-z
11. L. Jiang, C. Tao, A. He, X. He.

Overexpression of miR-126 sensitizes osteosarcoma cells to apoptosis induced by epigallocatechin-3-gallate. *World J Surg Oncol.*, 12, 383 (2014)  
DOI: 10.1186/1477-7819-12-383

12. K. M. Kyeong, J. S. Bong, K. Jong-Sik, R. Mee Sook, L. J. Hyun, L. Eun Hee, L. Hyoun Wook. Expression of microRNA miR-126 and miR-200c is associated with prognosis in patients with non-small cell lung cancer. *Virchows Arch.*, 465, 463-471 (2014)  
DOI: 10.1007/s00428-014-1640-4

13. C. Hongxia, L. Lingmin, W. Shaojun, L. Yupeng, G. Qi, L. Nonghua, Z. Xiaodong, C. Changyan. Reduced miR-126 expression facilitates angiogenesis of gastric cancer through its regulation on VEGF-A. *Oncotarget*, 5, 11873-11885 (2014)  
DOI: 10.18632/oncotarget.2662

14. W. Xiaohong, T. Shuang, L. Shu-Yun, L. Robert, J. S. Rader, M. Craig, Z. Zhi-Ming. Aberrant expression of oncogenic and tumor-suppressive microRNAs in cervical cancer is required for cancer cell growth. *PLoS One*, 3, e2557 (2008)  
DOI: 10.1371/journal.pone.0002557

15. Y. Tatsuro, I. Takeru, W. Rika, T. Keiichi, M. Hiroshi, N. Daisuke, N. Yujiro, M. Takeo, H. Shinichiro, M. Michiko. Underexpression of miR-126 and miR-20b in hereditary and nonhereditary colorectal tumors. *Oncology*, 87, 58-66 (2014)  
DOI: 10.1159/000363303

16. Li, Zeng, Li, Nan, Li, Xiayu, Wang, Xiaoyan, Wu, Minghua. Expression of miR-126 suppresses migration and invasion of colon cancer; cells by targeting CXCR4. *Mol Cell Biochem.*, 381, 233-242 (2013)  
DOI: 10.1007/s11010-013-1707-6

17. A. Salajegheh, H. Vosgha, M. A. Rahman, M. Amin, R. A. Smith, K. Y. Lam. Interactive role of miR-126 on VEGF-A and progression of papillary and undifferentiated thyroid carcinoma. *Hum Pathol.*, 51, 75-85 (2016)  
DOI: 10.1016/j.humpath.2015.12.018

18. X. Yin, K. Shweta, M. A. Zeiger, Z. Lisa, K. Electron. miR-126-3p Inhibits Thyroid Cancer Cell Growth and Metastasis, and Is Associated with Aggressive Thyroid Cancer. *Plos One*, 10, e0130496 (2015)  
DOI: 10.1371/journal.pone.0130496

19. W. Qiang, Z. Jie, B. Lin, W. Tongtong, Z. Haishan, M. Qingjie. miR-126 inhibits papillary thyroid carcinoma growth by targeting LRP6. *Oncol Rep.*, 34, 2202-2210 (2015)  
DOI: 10.3892/or.2015.4165

20. Y. Song, J. Sun, J. Zhao, Y. Yang, J. Shi, Z. Wu, X. Chen, G. Peng, Z. Miao, Z. Wang. Non-coding RNAs participate in the regulatory network of CLDN4 via ceRNA mediated miRNA evasion. *Nat Commun.*, 8, 289 (2017)  
DOI: 10.1038/s41467-017-00304-1

21. W. Chen, R. Zheng, P. D. Baade, S. Zhang, H. Zeng, F. Bray, A. Jemal, X. Q. Yu, J. He. Cancer statistics in China, 2015. *Ca Cancer J Clin.*, 66, 115-132 (2016)  
DOI: 10.3322/caac.21338

22. J. J. Sancho, T. W. J. Lennard, I. Paunovic, F. Triponez, A. Sitges-Serra. Prophylactic central neck dissection in papillary thyroid cancer: a consensus

report of the European Society of Endocrine Surgeons (ESES). *Langenbecks Arch Surg*, 399, 155-163 (2014)  
DOI: 10.1007/s00423-013-1152-8

23. Z. Zhu, S. Du, K. Yin, S. Ai, M. Yu, Y. Liu, Y. Shen, M. Liu, R. Jiao, X. Chen, W. Guan. Knockdown long noncoding RNA nuclear paraspeckle assembly transcript 1 suppresses colorectal cancer through modulating miR-193a-3p/KRAS. *Cancer Med*. 8:261-275 (2018)  
DOI: 10.1002/cam4.1798

24. H. Tan, L. Zhao. lncRNA nuclear-enriched abundant transcript 1 promotes cell proliferation and invasion by targeting miR-186-5p/HIF-1alpha in osteosarcoma. *J Cell Biochem*, 120, 6502-6514 (2019)  
DOI: 10.1002/jcb.27941

25. R. Garzon, G. A. Calin, C. M. Croce. MicroRNAs in Cancer. *Annu Rev Pathol.*, 60, 167-179 (2009)  
DOI: 10.1146/annurev.med.59.053006.10470  
7

26. W. Xu, A. S. Lucas, Z. Wang, Y. Liu. Identifying microRNA targets in different gene regions. *BMC Bioinformatics.*, 15, 1-11 (2014)  
DOI: 10.1186/1471-2105-15-S7-S4

27. F. Ebrahimi, E. Al. miR-126 in human cancers: clinical roles and current perspectives. *Exp Mol Pathol.*, 96, 98-107 (2014)  
DOI: 10.1016/j.yexmp.2013.12.004

Abundant Transcript 1; lncRNAs; long-chain non-coding RNAs; EMT, epithelial-mesenchymal transition

**Key Words:** Thyroid carcinoma, Nuclear Enriched Abundant Transcript 1, miR-126, tumorigenesis, VEGFA

**Send correspondence to:** Xuemei Wu, Department of Endocrinology, Rui'an People's Hospital and The Third Affiliated Hospital of Wenzhou Medical University, Jiyun mountain road, Anyang street, Ruian, Zhejiang, 325200, P. R. China, Tel: 86-13906646000, Fax: 0577-65866339, E-mail: z53xb5zj@sina.com

**Abbreviation:** TC, thyroid carcinoma; PTC, Papillary thyroid carcinoma; ATC, Anaplastic thyroid cancer; NEAT1, Nuclear Enriched